

Pressure broadening and fine-structure-dependent predissociation in oxygen $B^3\Sigma_u^-, v=0$

Sandro Hannemann,^{a)} GuoRong Wu, Eric-Jan van Duijn, and Wim Ubachs^{b)}
Laser Centre, Vrije Universiteit, De Boelelaan 1081, 1081 HV Amsterdam, The Netherlands

Philip C. Cosby
Molecular Physics Laboratory, Stanford Research Institute (SRI) International, Menlo Park, California 94025

(Received 16 June 2005; accepted 20 September 2005; published online 3 November 2005)

Both laser-induced fluorescence and cavity ring-down spectral observations were made in the Schumann-Runge band system of oxygen, using a novel-type ultranarrow deep-UV pulsed laser source. From measurements on the very weak (0,0) band pressure broadening, pressure shift, and predissociation line-broadening parameters were determined for the $B^3\Sigma_u^-, v=0, F_i$ fine-structure components for various rotational levels in O_2 . The information content from these studies was combined with that of entirely independent measurements probing the much stronger (0,10), (0,19), and (0,20) Schumann-Runge bands involving preparation of vibrationally excited O_2 molecules via photolysis of ozone. The investigations result in a consistent set of predissociation widths for the $B^3\Sigma_u^-, v=0$ state of oxygen. © 2005 American Institute of Physics. [DOI: 10.1063/1.2118507]

I. INTRODUCTION

The oxygen Schumann-Runge (SR) band system is an extremely important absorption system for the radiation budget and the chemistry of the Earth's atmosphere. Photoabsorption via the SR bands controls the penetration depth of deep-UV radiation into the lower levels of the atmosphere and its interaction with other molecules such as N_2O , H_2O , HNO_3 , and fluorocarbons.¹ Near 200 nm, where the SR bands of O_2 are weak, and the absorption by ozone is weak as well, the $1/e$ value of radiation penetrating into the Earth's atmosphere lies in the stratosphere. Predissociation via the upper $B^3\Sigma_u^-$ state in oxygen molecules is the source of ground-state atomic oxygen (3P) in the atmosphere above 60 km. In view of their atmospheric relevance detailed quantitative studies into the finest details of the predissociation phenomena in O_2 ($B^3\Sigma_u^-$) are warranted.

On the experimental side Lewis *et al.* have investigated predissociation phenomena for the main isotopomer,² for $^{16}O^{18}O$,³ and for $^{18}O_2$.⁴ Cheung *et al.* have also determined predissociation linewidths for bands (1,0) to (12,0) in $^{16}O_2$ (Ref. 5) as well as for the $^{16}O^{18}O$ and $^{18}O_2$ species.⁶ Yang *et al.*⁷ investigated predissociation in $v'=10-11$ levels by monitoring laser-induced fluorescence. There have been numerous theoretical studies on the nature of the predissociation mechanism, where most of the work is based on the initial framework developed by Julienne.⁸ Cheung and co-workers performed calculations to unravel the rotational, vibrational, isotopic, and fine-structure effects on the rates of dissociation.⁹⁻¹² Alternative calculations on all details pertaining to the predissociation widths including fine-structure dependencies were performed by Lewis *et al.*¹³ An extensive

and comparative study on the predissociation was performed combining data from laser-induced fluorescence spectroscopy, high-resolution absorption, and vacuum ultraviolet (vuv)-Fourier-transform spectroscopy.¹⁴ Finally, *ab initio* calculations on the predissociation mechanism in O_2 were undertaken by Li *et al.*¹⁵

In most studies the lowest $B^3\Sigma_u^-, v'=0$ level, which is the least subject to predissociation, was not included because the Franck-Condon factor for excitation from the $X^3\Sigma_g^-, v''=0$ ground vibrational level, in the weak (0,0) band is very small (at the 10^{-9} level). Cosby *et al.*¹⁶ were able to investigate the $B^3\Sigma_u^-, v=0$ state through a scheme, where O_2 in the $v=9, 10$, and 21 levels of the $X^3\Sigma_g^-$ ground state was prepared via laser photolysis of ozone. This has the advantages that Franck-Condon factors for the bands probing $B^3\Sigma_u^-, v=0$ are largely increased and the spin splittings in the corresponding bands are favorably enlarged.

In the present study new information is obtained on the predissociation properties of the $B^3\Sigma_u^-$ upper state, with a special focus on the lowest $v'=0$ vibrational level. New measurements performed at the Amsterdam Laser Centre are combined with remeasurements at Stanford Research Institute (SRI) following the experimental scheme of Ref. 16. The bandwidth of the deep-UV laser excitation source used in Amsterdam (100 MHz or 0.003 cm^{-1}) is so narrow, that the true molecular line shape can be determined, resulting from Doppler, predissociation, and collisional widths. These linewidth measurements are an extension to a spectroscopic study on the (0,0) and some other bands that have been published separately.¹⁷ From a comparison of relative line intensities obtained in cavity-ring-down (CRD) measurements and laser-induced fluorescence (LIF) information on fine-structure-dependent predissociation rates is obtained. Also from a detailed analysis of the spectral line shape of the singly resolved $P_1(1)$ line in the $B^3\Sigma_u^- - X^3\Sigma_g^-(0,0)$ band a

^{a)}Electronic mail: sandro@nat.vu.nl

^{b)}Electronic mail: wimu@nat.vu.nl

pressure broadening and a pressure shift coefficient could be determined. It is for the first time that these collisional effects are observed in the $B^3\Sigma_u^-, v=0$ state; the results are, however, in good agreement with previous works on higher v' levels.^{18,19}

In the SRI experiments, the O_2 is prepared in excited vibrational levels and probed by a narrow-band tunable laser. LIF spectra were recorded for the (0,10), (0,19), and (0,20) bands using the fundamental and second harmonics, respectively, of the tunable dye laser. The advantage of probing the $B^3\Sigma_u^-$ state from the excited vibrational levels of the $X^3\Sigma_g^-$ ground state are twofold. First, much lower photon energies are required to access the $B^3\Sigma_u^-, v=0$ level, with a corresponding decrease in the Doppler broadening of the transitions. Second, the $B^3\Sigma_u^-, v=0$ level can be probed in more than one band, each with a different spacing of the rotational and fine-structure lines. The present measurements thus yield three independent sets of $B^3\Sigma_u^-, v=0$ predissociation widths.

II. EXPERIMENT

A. Amsterdam setup and measurements

Two different spectroscopic techniques were applied for the investigation of the (0,0) Schumann-Runge band absorbing in the deep UV. In both configurations a pulsed titanium:sapphire laser system is employed, the output of which is frequency converted to its fourth harmonic to reach deep-UV wavelengths. This laser source has a bandwidth of 0.003 cm^{-1} and is tunable in the relevant range near 202 nm. All spectra were recorded at rather moderate laser-pulse energies of less than 0.15 mJ/pulse; in the CRD experiments only a minute fraction of this energy is coupled into the resonator. Further details were given in Ref. 20.

Cavity ring-down spectroscopy (CRDS) was performed in a cell of length 80 cm and a diameter of 1 cm, similar as in a previous study on one of the weaker visible band systems.²¹ The optical cavity, spanning the entire cell length, is formed by two reflective mirrors with $R \approx 97\%$ in the range of 197–203 nm and radius of curvature of 1 m. CRD recordings were performed at gas pressures in the range of 30–300 mbars, where the pressure was monitored online on a baratron. The methods for monitoring and evaluating the CRD transients, and retrieving the absorption spectrum, were described previously.²⁰

Laser-induced fluorescence measurements were also performed at pressure conditions of 30–300 mbars in a static gas cell. Fluorescence is collected by a mirror-lens system and filtered by a number of colored filters transmitting a broad wavelength band near 300 nm, where fluorescence originating in the $O_2 B^3\Sigma_u^-, v'=0$ state is expected. In view of power fluctuations during a scan the LIF spectra are normalized to deep-UV-laser intensity probed on a photodiode.

Absolute wavelength calibration, in particular, for the collisional shift measurements, was performed by using an ATOS wavelength meter, giving an accuracy of 200 MHz or 0.006 cm^{-1} at deep-UV wavelengths. Relative frequency spacings as well as linewidths were determined by comparing to transmission fringes of an etalon, yielding an even better precision on a relative scale.

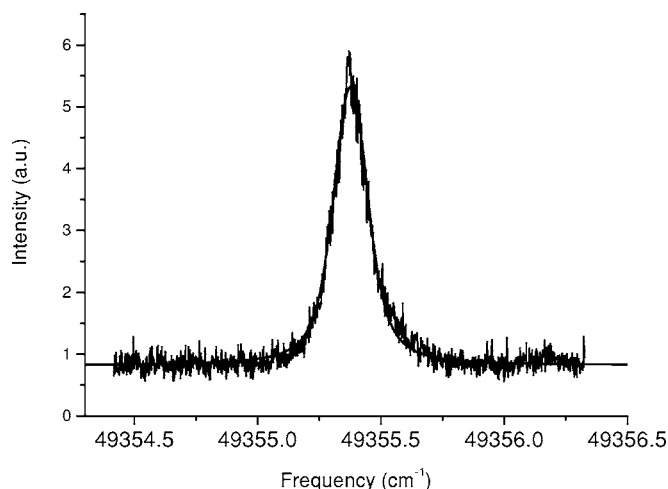


FIG. 1. Spectral recording of the single rotationally resolved $P(1)$ line of the $B^3\Sigma_u^-X^3\Sigma_g^-(0,0)$ band in $^{16}O_2$ at 38 mbars. Detection by LIF.

B. SRI setup and measurements

The $B^3\Sigma_u^-, v=0$ LIF bands were recorded as a by-product of previously reported measurements of the higher vibrational levels in the $B^3\Sigma_u^-$ state.¹⁴ The experimental details relevant to those measurements are given in Ref. 14 and details of the general technique and analysis are given in Ref. 16, so only the general features of the experiments are summarized here. Two laser beams are used in the SRI configuration: (1) a strong pump laser (4 mJ at 280 nm) dissociates O_3 in a 2% mixture of O_3 in He at 40 mbars, to produce vibrationally excited O_2 and (2) a collinear, temporally delayed (10–30 μs), weak (0.5–5 μJ), tunable probe laser excites the $B^3\Sigma_u^-X^3\Sigma_g^-$ transition in a single-photon absorption from one of the excited vibrational levels. The $O_2 B^3\Sigma_u^-$ fluorescence is monitored by a photomultiplier, again after transmission through a filter centered at 350 nm [full width at half maximum (FWHM)=50 nm]. The (0,19) and (0,20) bands were probed using the fundamental of the LPD3000E laser operating with Exalite 428 or Coumarin 440 dye and wavelength calibrated by simultaneously recording the Te_2 absorption spectrum. The (0,10) band was probed using the second harmonic of this laser operating with Rhodamine 6G dye and the fundamental was wavelength calibrated by simultaneously recording the LIF spectrum of I_2 vapor.

III. PRESSURE EFFECTS

Both pressure and collisional effects on the one hand and predissociation phenomena on the other give rise to line broadening on individual spectral lines. The analysis of these phenomena is therefore intertwined, and at the same time complicated by the fact that each spectral structure consists of three unresolved spin components. The $P_1(1)$ transition is a fortunate exception to this rule; it appears as a single resolved fine-structure component probing the $N=0, J=1, F_1$ fine-structure level.¹⁷ A systematic study was performed of the line broadening of this single component. An example of a spectral recording, using the LIF technique at a pressure of 38 mbars, is shown in Fig. 1. Similar recordings were performed in the pressure range of 0–300 mbars.

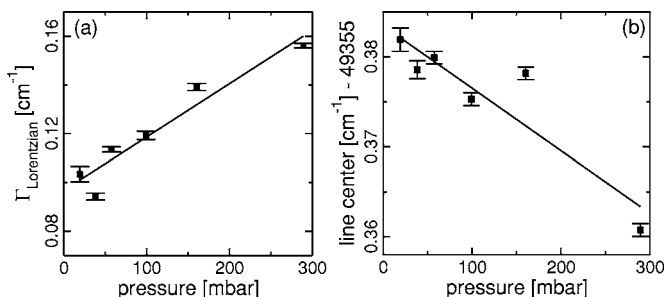


FIG. 2. (a) The combined effect of collisional broadening and predissociation as observed on the $P(1)$ line of the $B^3\Sigma_u^- - X^3\Sigma_g^-(0,0)$ band in $^{16}\text{O}_2$. Lorentzian contribution to the linewidth after deconvolution of the observed profile with a Doppler component (Gaussian profile) of 0.107 cm^{-1} (FWHM). (b) Collisional shift effect as observed on the $P(1)$ line of the $B^3\Sigma_u^- - X^3\Sigma_g^-(0,0)$ band in $^{16}\text{O}_2$.

The line shapes of these recordings were analyzed taking into account that they all undergo Doppler broadening, which for the O_2 molecule at 200 nm amounts to $\Delta_D = 0.107\text{ cm}^{-1}$ (FWHM). A Gaussian function of width Δ_D was convolved with a Lorentzian function of width Γ_L and the deviations from the resulting function were minimized in a fitting routine to extract the Lorentzian contribution to the line broadening. The resulting values from this numerical procedure to derive a value for the total Lorentzian contribution Γ_L are plotted in Fig. 2. Physically this Γ_L represents the combined effect of predissociation and collisional broadening. Both phenomena cause homogeneous line broadening and a Lorentzian line shape. A mathematical property of Lorentzian functions is the simple rule of additivity of their widths upon convolution, while the convoluted function is again a Lorentzian.

This makes it possible to disentangle the contributions of both physical phenomena in a simple manner: the slope in Fig. 2 represents the collisional broadening effect, assumed to be linear in pressure p , while the intercept at $p=0$ yields the value for the predissociation broadening Γ_{pred} . A linear fit to the pressure-dependent data, using the function

$$\Gamma_L = \Gamma_{\text{pred}} + \Gamma_{\text{col}} p \quad (1)$$

yields a value for the predissociation broadening,

$$\Gamma_{\text{pred}} = 0.097 \pm 0.002\text{ cm}^{-1}, \quad (2)$$

for the $v'=0, N=0, J=1$ state, and a value for the collisional parameter for the same state,

$$\Gamma_{\text{col}} = (2.2 \pm 0.3) \times 10^{-4}\text{ cm}^{-1}/\text{mbar}. \quad (3)$$

The same spectral recordings for the singly resolved $P_1(1)$ line in the (0,0) band were also used to assess collisional shifts in the Schumann-Runge band system. In the fits line centers were determined as displayed in Fig. 2. From a fit of the slope to the data in Fig. 2 a collisional shift parameter was determined at

$$\delta_{\text{shift}} = (-7 \pm 2) \times 10^{-5}\text{ cm}^{-1}/\text{mbar}. \quad (4)$$

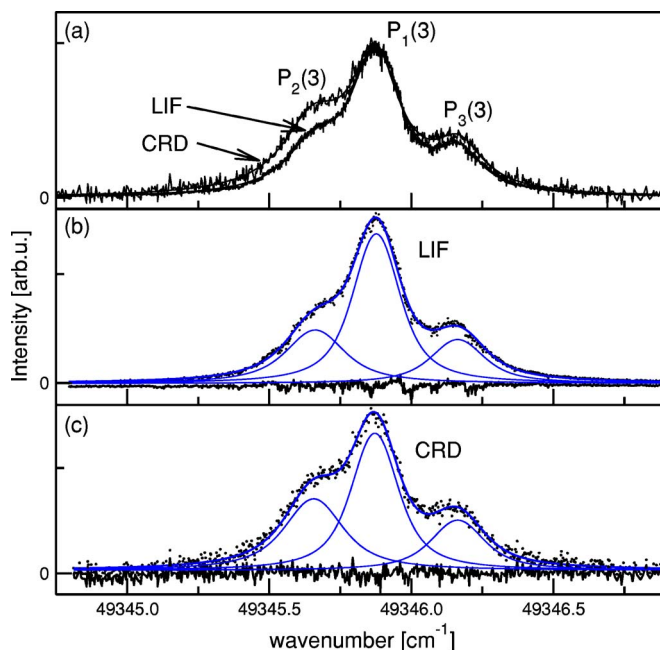


FIG. 3. Spectral recordings of the three fine structure components of the $P(3)$ line of the $B^3\Sigma_u^- - X^3\Sigma_g^-(0,0)$ band in $^{16}\text{O}_2$, both by CRD spectroscopy and by LIF at a pressure of 300 mbars. Panel (a) gives direct proof for the more rapid predissociation of F_2 and F_3 components, with respect to F_1 . Panel (b) shows the resulting fit for the spectral LIF profile using parameters $\Gamma(F_i)$, as described in the text. Panel (c) shows the resulting fit to the CRD profile. In the lower panels the calculated contributions of each fine-structure component F_i are plotted, as well as residuals between experimental and calculated profiles.

IV. FINE-STRUCTURE-DEPENDENT PREDISSOCIATION FROM MEASUREMENTS IN THE (0,0) BAND

In Fig. 3 typical recordings of the $P(3)$ line of the (0,0) band in $^{16}\text{O}_2$ are displayed, obtained by LIF and by CRD. Both spectra were recorded at a pressure of 300 mbars. The spectra of the $P(5)$ triplet were obtained in the same way. In $P(N)$ transitions for higher N values as well as in the R branch the spin splittings are too small for the intensities for the three individual components to be disentangled.

The rationale of a comprehensive analysis, using the information contained in both spectra, is as follows. In both detection methods the linewidths of the individual fine-structure components are determined by Doppler broadening, collisional broadening, and predissociation broadening. Since the spectra were obtained from samples at 300 mbars in both cases the individual line shape and width of the F_i components are the same, while the relative intensities for the fine-structure components will differ in both spectra. In the fitting procedures a Gaussian profile of a width fixed to the Doppler broadening of 0.107 cm^{-1} was convolved with three variable Lorentzian contributions $\Gamma(F_i)$. The Lorentzian components to the width represent a variable predissociation width and a constant contribution of 0.066 cm^{-1} (FWHM) associated with a pressure of 300 mbars; this value follows from the previous analysis on the $P_1(1)$ line and will finally be subtracted from the obtained fit results. The difference between the two detection methods is in the intensities; in fact we only use the information on the relative intensities

between fine-structure components in each individual spectrum. Since CRD is a method probing direct absorption, the relative intensities for the spectral fine-structure components should follow the theoretical line strengths; hence in the fit on the CRD spectrum the relative intensities were kept fixed at the values as expected from the Hönl-London factors and room-temperature Boltzmann factors. For the $P(3)$ line, that is, $P_3(3)/P_1(3)=0.427$ and $P_2(3)/P_1(3)=0.683$ and for the $P(5)$ line $P_3(5)/P_1(5)=0.651$ and $P_2(5)/P_1(5)=0.804$.

While CRD measures in fact direct absorption, and therewith probes the excitation oscillator strength, in LIF detection excitation strength and fluorescence yield both affect the intensity. In the latter scheme the fluorescence intensity is reduced due to competition with predissociation. The collisional effects giving rise to the additional line broadening, as studied in the above for the $P(1)$ line, may give rise to quenching of the fluorescence and affect the intensities obtained in the LIF study. However, that depends on the nature of the collisional processes and detailed information for such phenomena is lacking for the Schumann-Runge band systems. The collisional effects may be related to elastic scattering, to rotational or vibrational energy transfer within the $B^3\Sigma_u^-$ state, or to collisional transfer to continuum states.

Considering the competition of predissociation and fluorescence, Fig. 3 shows in a qualitative but direct manner that the F_2 and F_3 components are more rapidly predissociated than the F_1 component. If it is assumed that the radiative lifetime is 50 ns,^{16,22} then the fluorescence yield is on the order of 0.1% for a predissociation width of 0.1 cm^{-1} . Thus the fluorescence rate k_{rad} is much smaller than the collisional decay rate k_{col} and the predissociation decay rate k_{pred} . Note that total decay rates k_{tot} relate to (Lorentzian) contributions Γ_L via $k_{\text{tot}}=k_{\text{col}}+k_{\text{pred}}+k_{\text{rad}}=2\pi\Gamma_L$. Furthermore it can be shown that the relative fluorescence intensities $(F_i/F_j)_{\text{LIF}}$ can be expressed in terms of the relative absorption intensities $(F_i/F_j)_{\text{ABS}}$, via

$$\left(\frac{F_i}{F_j}\right)_{\text{LIF}} = \left(\frac{F_i}{F_j}\right)_{\text{ABS}} \frac{k_j^{\text{tot}}}{k_i^{\text{tot}}}, \quad (5)$$

where the $k_{i,j}^{\text{tot}}$ factors relate to the total decay rates of the excited states, including the collisional effects. Equation (5) is valid, whether or not secondary fluorescence due to collision-induced inelastic scattering within the $B^3\Sigma_u^-$, v, N, J manifold plays a role.

The full information contained in both LIF and CRD spectra as displayed in Fig. 3, and similarly for the recording of the $P(5)$ triplet, is used in one comprehensive fitting analysis, that is constrained by Eq. (5). Hence the line strengths in the CRD and LIF spectra follow different constraints in the combined fits. It should be noted that all statements on intensities hold for *integrated* intensities. The fits using a combined set of parameters for both traces are shown in the lower panels of Fig. 3. There the observed and calculated spectra are displayed, as well as the calculated curves for the three fine-structure components. Also, displayed in a separate trace, are the deviations between observed and calculated spectra, demonstrating the quality of the procedure.

Resulting values for $\Gamma_{\text{pred}}(F_i)$ from the combined fits are reduced by 0.066 cm^{-1} to correct for the collisional broadening effect at 300 mbars.

V. LINE BROADENING IN THE (0,10), (0,19), AND (0,20) BANDS

At the very low pressure of O_3 (<1 mbar) in the He buffer gas, pressure broadening of the $B^3\Sigma_u^- - X^3\Sigma_g^-$ fluorescence spectra is negligible. The emission coefficient of the (0,20) band is 10^5 times larger than that of the (0,0) band. Those of the (0,19) and (0,10) bands are, respectively, factors of 3 and 40 times stronger than the (0,20). The essence of the experiment was to limit the power broadening in these SR bands, while retaining sufficient signal to noise to accurately measure the line profiles. To achieve the very low power densities required for these measurements, the LPD3000E was operated without its preamplifier and with a severely attenuated amplifier, at the cost of some degradation in the laser linewidth. In addition, the output beam was expanded by a factor of three or more to keep the effect of power broadening of the SR transitions to less than 10% for transitions terminating in the lower rotational levels. At the required low power levels, the (0,19) spectra yielded the poorest signal-to-noise ratios of the three bands. Probe laser bandwidths, estimated from the features in the wavelength calibration spectra, an external etalon, and from analysis of the LIF line profiles, were approximately 0.04 cm^{-1} for the (0,19) band, 0.1 cm^{-1} for the (0,20) band, and 0.07 cm^{-1} for the (0,10) band. In combination with the approximately room-temperature Doppler broadening, consistent with the rotational temperature of the rotational line intensities, the total inhomogeneous (Gaussian) contributions to the LIF peak shapes were 0.071, 0.122, and 0.125 cm^{-1} for the (0,19), (0,20), and (0,10) bands, respectively. Spectra are shown in Fig. 4 for the P - and R -branch lines in each band terminating in $N'=6$.

Analysis of the LIF spectra followed the procedure given in Ref. 14 using the Voigt line shape defined by Eqs. (4)–(7) of Ref. 16. These LIF line-shape equations include the dependence of fluorescence intensity on lifetime described by Eq. (5) above. The values of Γ_L obtained in the line fits, following a small correction for saturation broadening, are reported here as the predissociation level widths Γ_{pred} .

The determination of Γ_{pred} in the (0,20) band encompassed all main P - and R -branch lines with $N' < 26$. In the (0,10) band, coverage of the two main branches was complete for $N' < 18$, although the F_1 and F_2 components are effectively blended in both the P and R branches for $N' < 16$ –20. Coverage of the (0,19) band was much less extensive, with both P - and R -branch lines measured only at $N' = 2, 4, 6$, and 14. Γ_{pred} are reported here for $B^3\Sigma_u^-$, $v=0$ at $N'=0$ –20. From the combination of three bands and two branches for most levels, each of the values represents the average of at least three independent measurements, with six measurements contributing to most of the averages. For each of the bands, the differences in Γ_{pred} determined from the P and R lines terminating in a given N' were randomly distributed over a range of $\pm 10\%$. For the F_1 components, the dif-

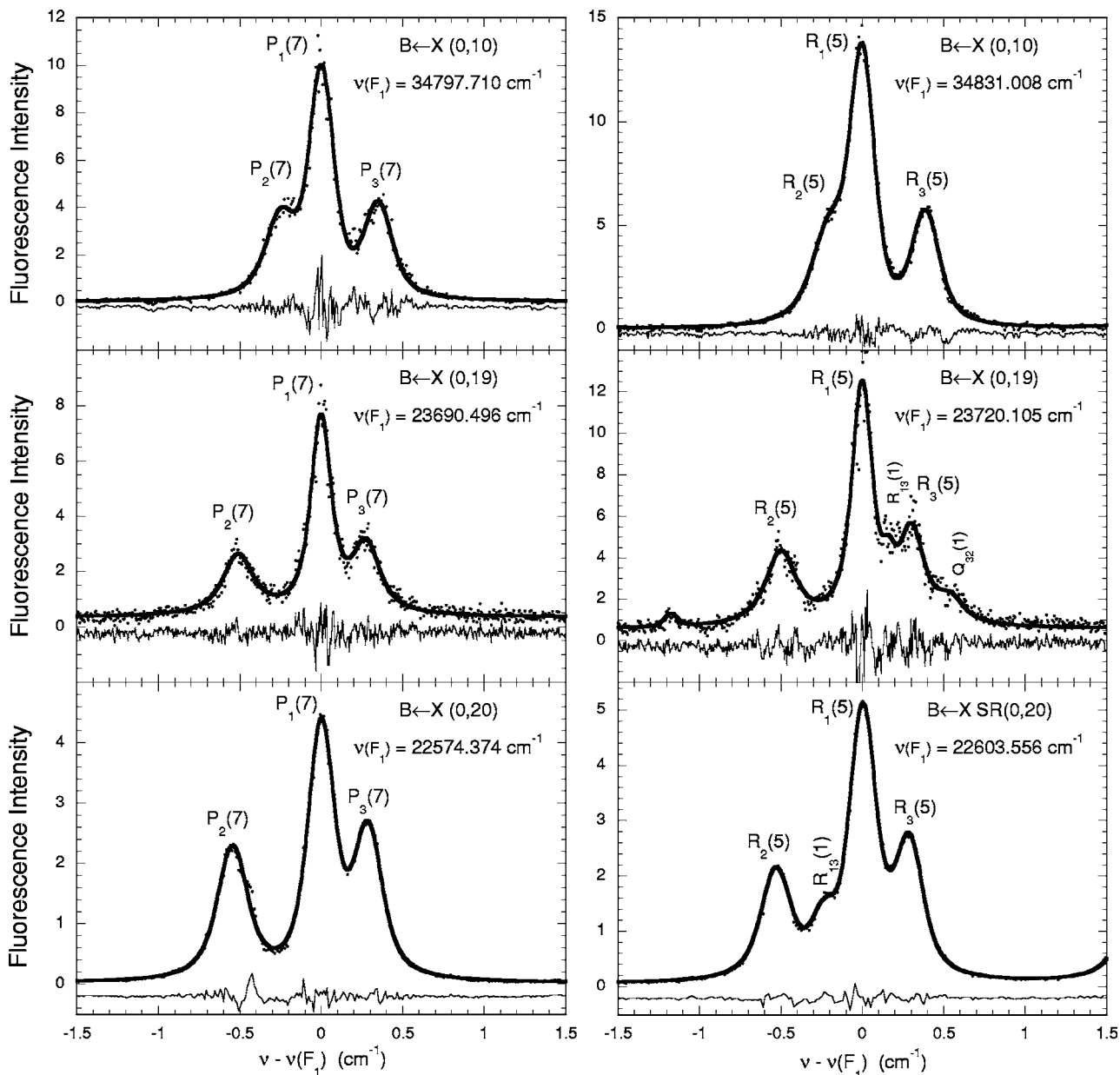


FIG. 4. SRI LIF spectral recordings (points) of the P - and R -branch lines terminating in the $N'=6$ levels of $B^3\Sigma_u^-, v=0$ for the (0,10), (0,19), and (0,20) Schumann-Runge bands. Fits to the transitions, including several weak satellite transitions, are given by the thick lines. The thin lines at the bottom of each spectrum show the residuals in the fits.

ferences in Γ_{pred} among the three bands were also consistent to within $\pm 10\%$. However, for the F_2 and F_3 levels, the values of Γ_{pred} determined from the three bands showed systematic deviations for levels $N' < 12$, where the values of Γ_{pred} from the (0,19) band were consistently larger by 26% for the F_2 levels and 29% for the F_3 levels, than those obtained from the other two bands. Apart from the lower signal-to-noise ratios in the (0,19) band and its relatively scant coverage, no specific reason for the larger Γ_{pred} values in this band could be identified. Consequently, we consider these larger values to be characteristic of the measurement errors and used all three bands to determine the average values of Γ_{pred} and their uncertainties for the $B^3\Sigma_u^-, v=0$ levels. The resulting predissociation level widths Γ_{pred} are shown by the points in Fig. 5, where the error bars represent one standard deviation in the uncertainty of the values.

VI. DISCUSSION AND CONCLUSION

There is a vast literature on the predissociation in the Schumann-Runge bands²⁻¹⁶ reflecting the importance of oxygen dissociation from a theoretical as well as an atmospheric perspective. The present findings on a fine-structure-dependent predissociation rate are well documented and are supported by the theoretical models of Lewis *et al.*¹³ and Tong *et al.*,¹² showing that the F_1 is the least predissociated and that the F_2 component is the most strongly affected by predissociation.

A study of the lowest vibrational level of the $B^3\Sigma_u^-$ state in oxygen has been performed by combining input from independent measurement schemes executed at different laboratories. In their combination the procedures represent the state of the art and the resulting values for the predissocia-

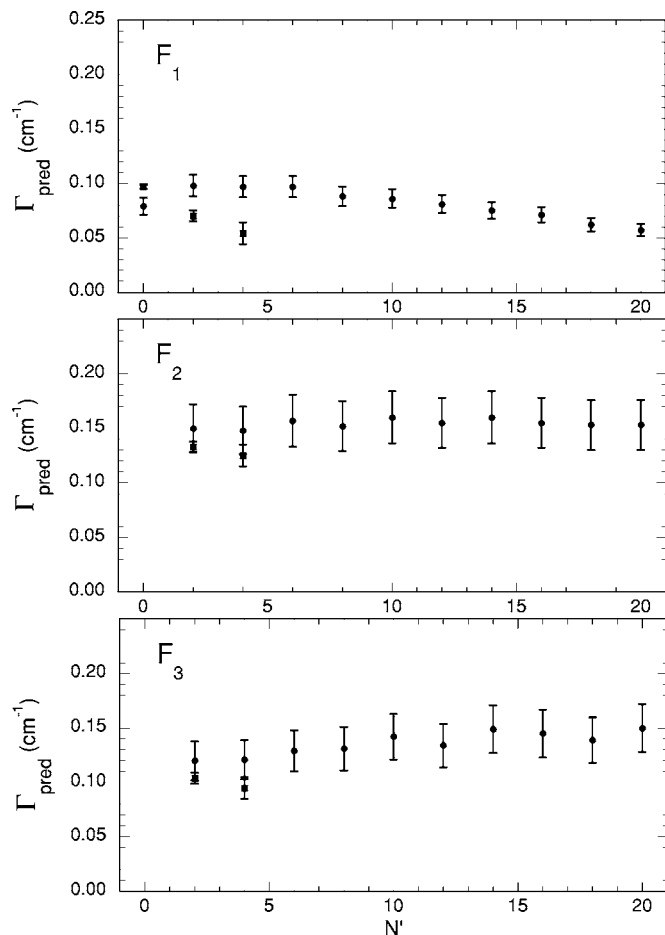


FIG. 5. Predissociation widths Γ_{pred} measured for the $B^3\Sigma_u^-, v=0, N, F_i$ fine structure levels in O_2 . Points=SRI. Squares=Amsterdam.

tion widths of the fine-structure levels in $B^3\Sigma_u^-, v=0$ form benchmark results for testing theoretical models of predissociation in O_2 . Previously discrepancies between rather strongly deviating findings obtained with different techniques in different laboratories have been addressed before with the aim of resolving them.^{13,14}

The present investigations produce reasonable, but yet not perfect, agreement between findings of different laboratories. The remaining deviations may be considered to represent the true level of experimental accuracies, and may be associated with the different compromises troubling the experimental approaches: the requirement of relatively high pressures in the Amsterdam setup, resulting in relatively large collisional contributions to the linewidths, and the delicate balance between signal intensity and saturation in the SRI experiments, and the necessary methods of deconvolution in both experiments.

We note that improved use of the narrow-band laser source could be made when detecting in the collision-free and Doppler-free conditions of a molecular beam; in such case no deconvolution nor extrapolation to zero pressure would be required to determine predissociation linewidths. Unfortunately attempts to observe LIF signals in the $B-X(0,0)$ band in a molecular beam failed thus far, due to the extremely small Franck-Condon factor combined with the small fluorescence rate.

The present value for the collisional broadening constitutes an independent verification at low and atmospherically relevant pressures of the results of the Canberra group, first at high pressures up to 60 bars,¹⁸ and subsequently at subatmospheric pressures.¹⁹ The resulting averaged value of $0.208 \pm 0.004 \text{ cm}^{-1}/\text{bar}$, measured for excited states with $v' = 2-15$, is in excellent agreement with the present finding. The result on the collisional shift, here established for $v' = 0$ is in agreement with the finding of Dooley *et al.*¹⁹ of $-5.6 \pm 0.8 \times 10^{-5} \text{ cm}^{-1}/\text{mbar}$ for vibrational levels $v' = 13-15$.

ACKNOWLEDGMENTS

The authors wish to thank B.R. Lewis (Canberra) for discussions and advice. The Netherlands Foundation for Fundamental Research of Matter (FOM) and the Space Research Organisation Netherlands (SRON) are acknowledged for financial support. The stay of one of the authors (G.R.W.) (Dalian Institute of Chemical Physics) at the Laser Centre VU Amsterdam is supported by a collaborative project (98-CDP034) between the Netherlands Royal Academy of Sciences (KNAW) and the Chinese Academy of Sciences (CAS). The measurements at SRI were partially supported by a grant from the Atmospheric Sciences Division of the (US) National Science Foundation.

- ¹J. E. Rosenfield, *J. Atmos. Terr. Phys.* **57**, 847 (1995).
- ²B. R. Lewis, L. Berzins, J. H. Carver, and S. T. Gibson, *J. Quant. Spectrosc. Radiat. Transf.* **36**, 187 (1986).
- ³B. R. Lewis, L. Berzins, and J. H. Carver, *J. Quant. Spectrosc. Radiat. Transf.* **37**, 219 (1987).
- ⁴B. R. Lewis, L. Berzins, and J. H. Carver, *J. Quant. Spectrosc. Radiat. Transf.* **37**, 229 (1987).
- ⁵A. S.-C. Cheung, K. Yoshino, J. R. Esmond, S. S.-L. Chiu, D. E. Freeman, and W. H. Parkinson, *J. Chem. Phys.* **92**, 842 (1990).
- ⁶S. S.-L. Chiu, A. S.-C. Cheung, K. Yoshino, J. R. Esmond, D. E. Freeman, and W. H. Parkinson, *J. Chem. Phys.* **93**, 5539 (1990).
- ⁷X. Yang, A. M. Wodtke, and L. Hüwel, *J. Chem. Phys.* **94**, 2469 (1990).
- ⁸P. S. Julienne, *J. Mol. Spectrosc.* **63**, 60 (1976).
- ⁹S. S.-L. Chiu, A. S.-C. Cheung, M. Finch, M. J. Jamieson, K. Yoshino, and W. H. Parkinson, *J. Chem. Phys.* **97**, 1787 (1992).
- ¹⁰A. S.-C. Cheung, D. K.-W. Mok, M. J. Jamieson, M. Finch, K. Yoshino, A. Dalgarno, and W. H. Parkinson, *J. Chem. Phys.* **99**, 1086 (1993).
- ¹¹A. S.-C. Cheung, D. K.-W. Mok, K. Yoshino, W. H. Parkinson, M. J. Jamieson, A. Dalgarno, and M. S. Child, *J. Chem. Phys.* **103**, 2369 (1995).
- ¹²G. S. M. Tong, A. S.-C. Cheung, and M. J. Jamieson, *J. Chem. Phys.* **114**, 7969 (2001).
- ¹³B. R. Lewis, S. T. Gibson, and P. M. Dooley, *J. Chem. Phys.* **100**, 7012 (1994).
- ¹⁴P. M. Dooley *et al.*, *J. Chem. Phys.* **109**, 3856 (1998).
- ¹⁵Y. Li, H.-P. Liebermann, and R. J. Buenker, *J. Chem. Phys.* **114**, 10396 (2001).
- ¹⁶P. C. Cosby, H. Park, R. A. Copeland, and T. G. Slanger, *J. Chem. Phys.* **98**, 5117 (1993).
- ¹⁷S. Hannemann, E. J. van Duijn, and W. Ubachs, *J. Mol. Spectrosc.* **232**, 33 (2005).
- ¹⁸B. R. Lewis, L. Berzins, C. J. Dedman, T. T. Scholz, and J. H. Carver, *J. Quant. Spectrosc. Radiat. Transf.* **39**, 271 (1988).
- ¹⁹P. M. Dooley, K. Waring, S. T. Gibson, and K. G. H. Baldwin, *J. Quant. Spectrosc. Radiat. Transf.* **58**, 93 (1997).
- ²⁰M. Sneeep, S. Hannemann, E. J. van Duijn, and W. Ubachs, *Opt. Lett.* **29**, 1378 (2004).
- ²¹H. Naus and W. Ubachs, *J. Mol. Spectrosc.* **193**, 442 (1999).
- ²²B. R. Lewis and S. T. Gibson, *J. Chem. Phys.* **93**, 7532 (1990).